Analysis of Multilayer Interconnection Lines for a High-Speed Digital Integrated Circuit

YOSHIRO FUKUOKA, MEMBER, IEEE, QUI ZHANG, DEAN P. NEIKIRK, MEMBER, IEEE, AND TATSUO ITOH, FELLOW, IEEE

Abstract—**A general method for the analysis of multilayer interconnection lines is presented. This method is capable of predicting frequency dispersion of the transmission-line parameters and is useful for accurately investigating the coupling phenomena among adjacent lines and the input and output impedance relations.**

I. Introduction

IN A VERY HIGH-SPEED digital integrated circuit, it is important to know the effects of interconnection lines, such as delay time and coupling between different lines. To date, a number of approximation techniques have been used for analyses of these characteristics. For delay time, a distributed *RC* network approximation is a typical approach, and for coupling, a quasi-static capacitance and inductance calculation is used [1], [2]. However, as the speed of the signal in the IC chip is increased, the electromagnetic nature of the pulse transmission will eventually appear. For instance, at clock rates of 10 Gbits/s, the clock harmonics are well into the millimeter-wave range (30–300 GHz), and the electromagnetic properties of the interconnection lines become important [3].

This paper presents a tool for the analysis of such lines. The technique is based on the full-wave analysis, and has originally been developed for analyses of multilayered hybrid and monolithic microwave integrated circuits. The features of this method are as follows.

1) It is a comprehensive analysis. As such, all of the approximation techniques used to date are considered as the limiting case of this method.

2) It can handle any number of wires (or lines) located at any of the different-layer interfaces. No symmetry in the structure is required and the width of the wire is arbitrary. The thickness of the wire is assumed to be negligible.

Information about the transmission-line characteristics can then be used for describing the circuit parameters of a section of a coupled-line system. If losses due to the semiconductor substrate are to be considered, this method allows us to simply replace the ground plane with a lossy dielectric layer [4]. When poly-silicon is used as a conductor in the integrated circuit, we can include the loss of the conductor in the analysis to take its effect into account [5].

Manuscript received January 22, 1985; revised February 7, 1985. This work was supported in part by the Office of Naval Research under Contract N00014-79-0053 and in part by the U.S. Army Research Office under Contract DAAG29-81-K-0053. The paper is based on a presentation at the First International IEEE VLSI Multilevel Interconnection Conference, June 21–22, 1984, New Orleans, LA (*Proceedings* pp. 246–251).

Y. Fukuoka is with Uniden Satellite Technology Inc., 5-13-12 Ginza, Chuo-Ku, Tokyo, 104 Japan.

Q. Zhang, D. P. Neikirk, and T. Itoh are with the Department of Electrical and Computer Engineering, University of Texas at Austin, Austin, TX 78712.

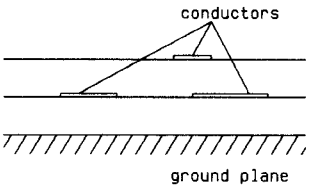

Fig. 1. Cross-sectional view of generalized coupled interconnection lines.

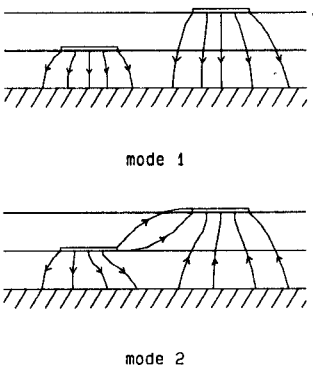

Fig. 2. Distribution of the electric field of the two different modes in a coupled two-line system.

II. Analysis

We use the spectral-domain method to determine the propagation constants and characteristic impedances [6]. Fig. 1 shows a general configuration of the multilayer interconnection lines. There exist as many modes as the number of lines located above the ground plane. These modes combine together and form the actual field around the lines, which satisfies all the input and output boundary conditions. An example is shown in Fig. 2. There are two fundamental modes existing in this two-line system which determine the phase delay and the cross-talk between two lines. The distribution of the electric field of the two modes are schematically shown in the figure. Mode 1 in the figure corresponds to an even mode in the symmetric structure, while mode 2 corresponds to an odd mode. The phase constants of these modes are calculated by solving an eigenvalue equation in the spectral domain. The character-

0018-9480/85/0600-0527$01.00 ©1985 IEEE

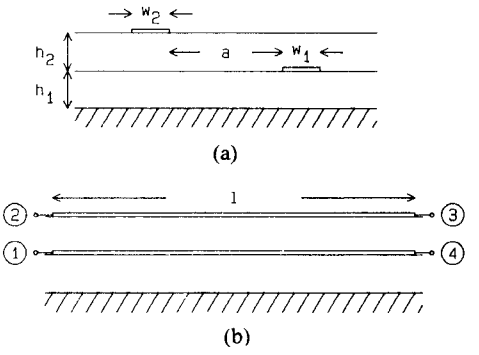

Fig. 3. A coupled two-line model used in the computation. (a) Cross-sectional view. (b) Side view. $w_1 = w_2 = h_1 = h_2 = 10$ μm, $a = 30$ μm, $l = 0.5$ mm.

istic impedances are defined through the following relation [7]:

$$Z_{ci} = \frac{2P_{\text{ave}}}{I_{zi}^2} = \frac{\int E_t \times H_i^* \, dS}{I_{zi}^2}$$

where P_{ave} is the average partial power associated with the line i and I_{zi} is the axial current in the line i. In the above, E_t is the total electric field and H_i the magnetic field created only by the current on the line i. Once the phase constants and the characteristic impedances of two modes are found, we can consider this coupled-line system as a black box and characterize it by network parameters such as an impedance matrix. The network parameters are given by a 4×4 matrix [8]. The matrix elements must be recalculated for each frequency since the phase constants and the characteristic impedances are frequency-dependent.

III. Computational Results

A two-line system as shown in Fig. 3 is chosen as a model for the numerical computations. Silicon dioxide (SiO_2, $\epsilon_r = 4$) is chosen for the dielectric material. Two metal strips are located on the different dielectric interfaces and are separated by 30 μm horizontally. First, the frequency dependence of the phase constants and the characteristic impedances are investigated. Fig. 4 shows the effective dielectric constants for the two independent modes. Mode 1, which is similar to an even mode of the symmetric lines, has faster phase velocity than mode 2. This indicates that the field around the lines spreads out of the dielectric layers. On the other hand, the effective dielectric constant of mode 2 is close to 4, which means the field is confined in the SiO_2 region, as expected for an "odd" mode. For this particular choice of structural parameters, the frequency dispersion appears at frequencies higher than 100 GHz, where the phase velocities of both modes become slower. The frequency dependence of the characteristic impedances is shown in Fig. 5, where Z_{cij} indicates the characteristic impedance of the line j of the mode i. The frequency dispersion is prominent for Z_{c22}. To confirm the accuracy of the results, we investigated how well the relation $Z_{c12}/Z_{c11} = Z_{c22}/Z_{c21}$ given in [8] is satisfied. We defined

$$\epsilon = |1 - Z_{c12}Z_{c21}/Z_{c11}Z_{c21}|.$$

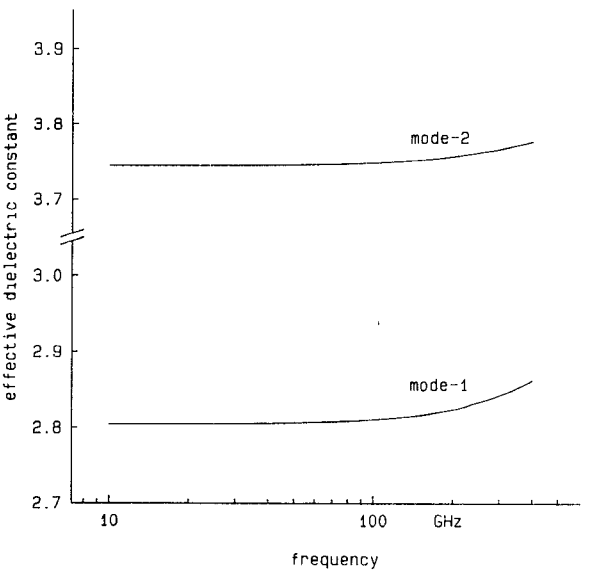

Fig. 4. Frequency dispersion of effective dielectric constants of two independent modes.

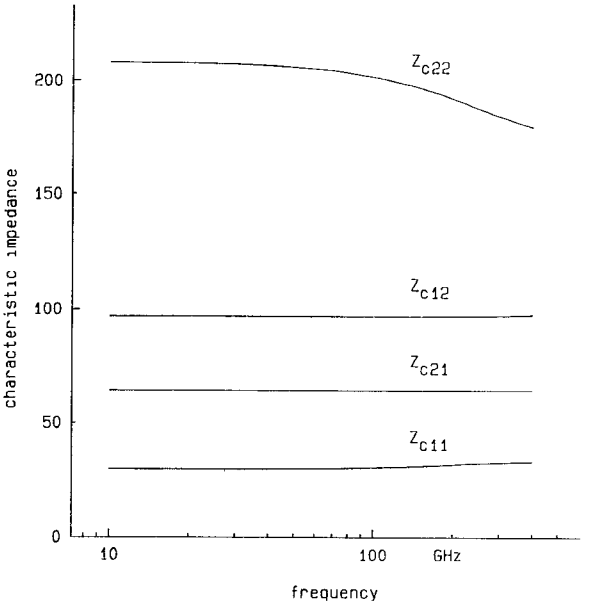

Fig. 5. Frequency dispersion of characteristic impedances: Z_{cij} is the characteristic impedance of line j of mode i.

For all the frequencies in Fig. 5, ϵ was found to be less than 0.01.

Using these results, we can now calculate network parameters of this coupled two-line system. Fig. 6 shows several elements of the 4×4 impedance matrix. The length of the lines are chosen to be 0.5 mm. All the matrix elements are purely imaginary because the structure is lossless. Since the structure is symmetric, there are several equal elements in the matrix, e.g., $Z_{11} = Z_{44}$, $Z_{12} = Z_{43}$, etc. All Z_{ii} elements become capacitive at low frequencies, while Z_{ij}, $i \neq j$, becomes inductive. For comparison, the quasi-static results from a conventional capacitance calculation are also shown in the figures as dotted lines. They are almost identical, but become slightly different at high frequencies because of the frequency dispersion as men-

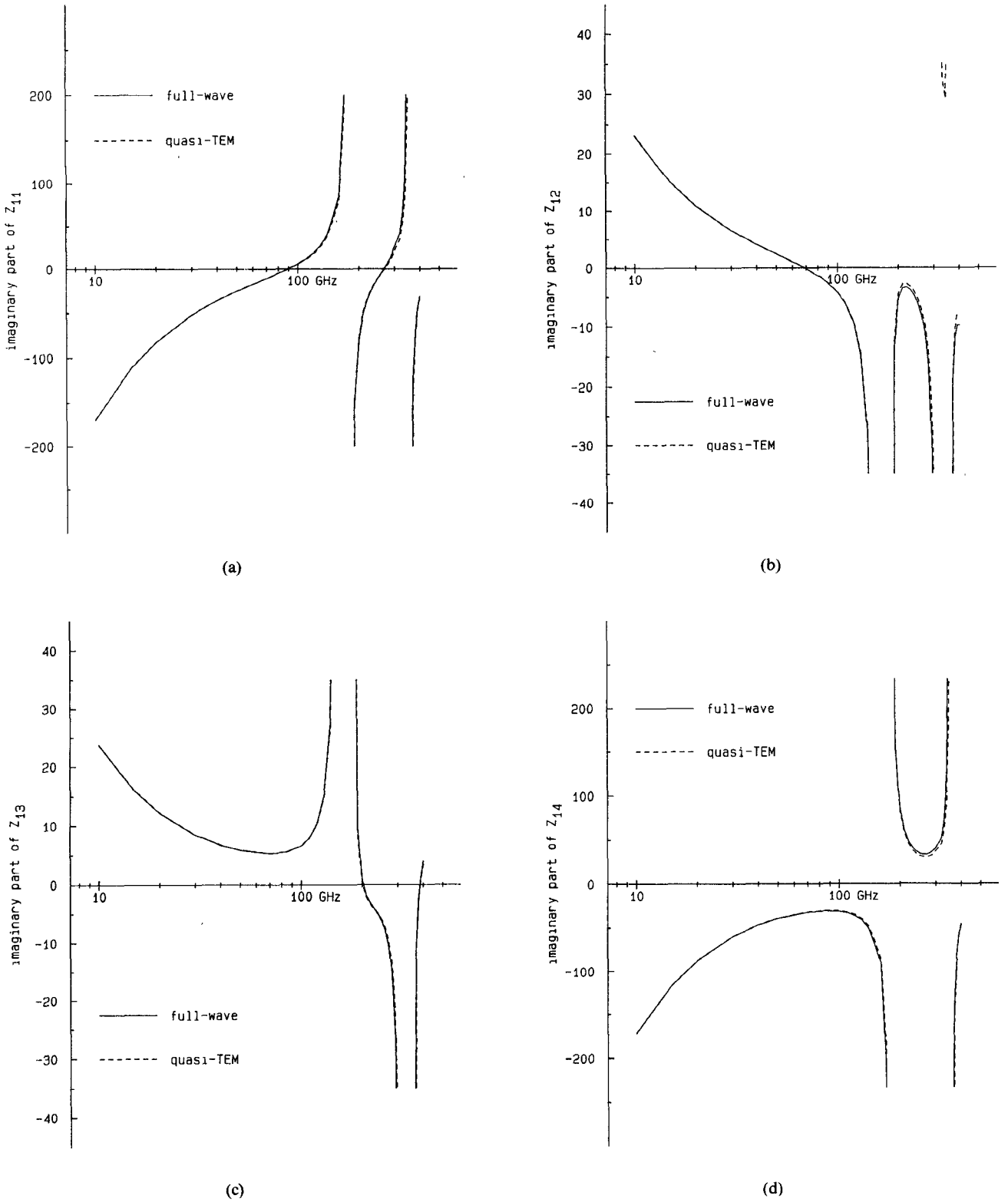

Fig. 6. Elements of an impedance matrix. (a) Z_{11}, (b) Z_{12}, (c) Z_{13}, (d) Z_{14}.

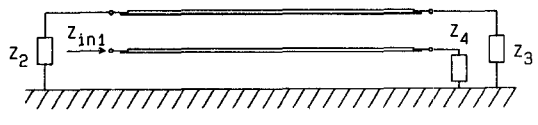

Fig. 7. Input impedance looking from port 1 when other ports are terminated by Z_2 through Z_4.

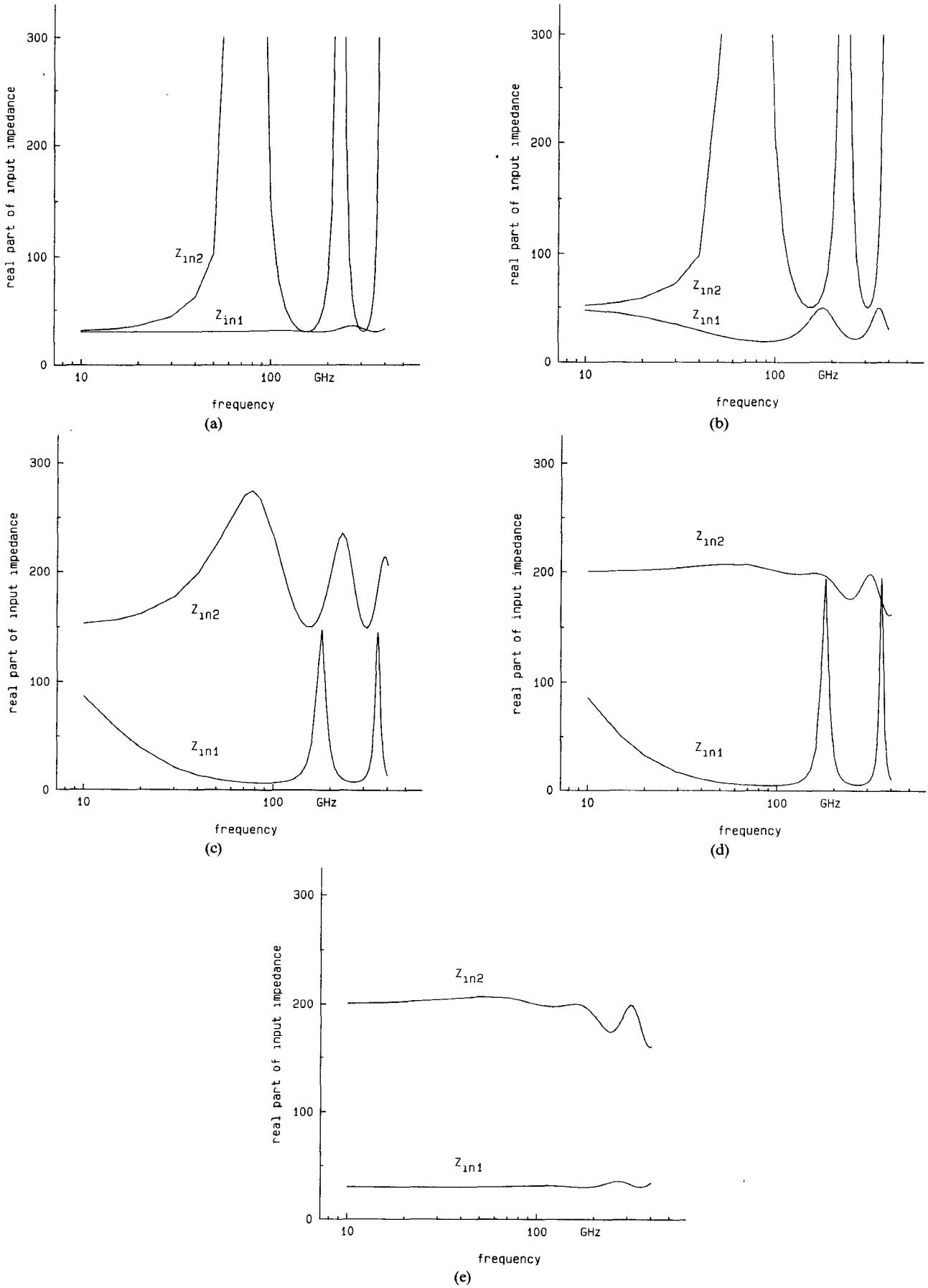

Fig. 8. Input impedances from port 1 (Z_{in1}) and port 2 (Z_{in2}). (a) $Z_1 = Z_2 = Z_3 = Z_4 = 30\ \Omega$. (b) $Z_1 = Z_2 = Z_3 = Z_4 = 50\ \Omega$. (c) $Z_1 = Z_2 = Z_3 = Z_4 = 150\ \Omega$. (d) $Z_1 = Z_2 = Z_3 = Z_4 = 200\ \Omega$. (e) $Z_1 = Z_4 = 30\ \Omega$, $Z_2 = Z_3 = 200\ \Omega$.

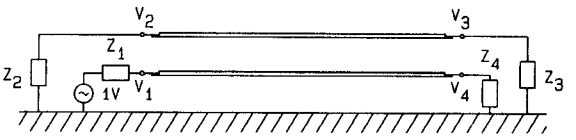

Fig. 9. Voltages at each port when ports 2 through 4 are terminated by Z_2 through Z_4 and a source with impedance Z_1 is connected to port 1.

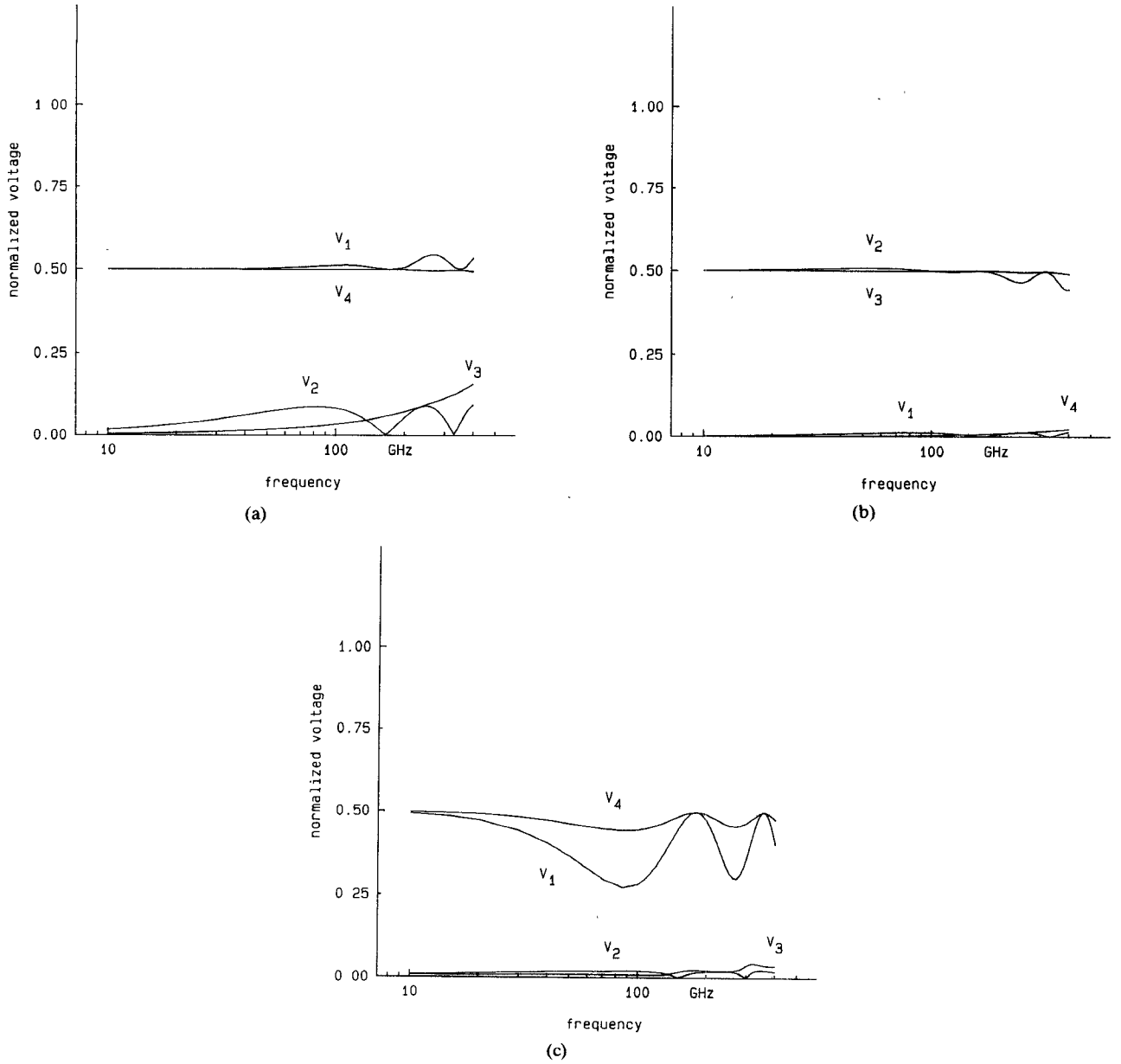

Fig. 10. Normalized voltages at each port. (a) 1-V source is connected at port 1. $Z_1 = Z_4 = 30\ \Omega$, $Z_2 = Z_3 = 200\ \Omega$. (b) 1-V source is connected at port 2. $Z_1 = Z_4 = 30\ \Omega$, $Z_2 = Z_3 = 200\ \Omega$. (c) 1-V source is connected at port 1. $Z_1 = Z_2 = Z_3 = Z_4 = 50\ \Omega$.

tioned above. In many practical applications, such small differences between the present full-wave and quasi-TEM analyses may not be important. However, it is important to recognize that such a fact cannot be found out until a full-wave calculation is performed.

The input impedances are also plotted with respect to the frequency. The input impedance looking from one port, while other ports are terminated by some impedances, are calculated (Fig. 7). In Fig. 8, the results are shown for different terminating impedances varying from 30 Ω to 200 Ω. When terminations are 30 Ω, the input impedance looking from port 1 appears to be almost constant over a wide range of frequency (Fig. 8(a)). The characteristic impedance of line 1 (lower line) of mode 1 (Z_{c11}) is about 30 Ω, and, therefore, this is the value required for the matching of line 1. On the other hand, the input impedance of port 2 is found to be almost constant when terminations are 200 Ω (Fig. 8(d)). This value corresponds to the char-

acteristic impedance of line 2 (upper line) of the mode 2 (Z_{22}). In this case, the input impedance of port 2 is affected by the large frequency dispersion of the characteristic impedance Z_{22}. When line 1 is terminated by 30 Ω and line 2 by 200 Ω, the input impedances of both ports 1 and 2 are constant over the frequency (Fig. 8(e)). As a consequence, the characteristic impedances Z_{c11} and Z_{c22} take important roles in matching conditions.

Finally, the relationships between the terminal voltages are investigated (Fig. 9). In Fig. 10(a), the voltages of all four ports are calculated and plotted with respect to frequency. Ports 2 and 3 are terminated by 200 Ω and port 4 is terminated by 30 Ω. At port 1, a source voltage with an internal impedance of 30 Ω is connected. As the figure shows, the voltage of port 4 is constant over the frequency. Relatively large voltages appear at ports 2 and 3, which indicates large crosstalk. In Fig. 10(b), a 200-Ω source is connected at port 2. In this case, the crosstalk is smaller, which is probably because of the larger impedance level of the upper line. Fig. 10(c) shows the voltage relationships when all ports are terminated by 50 Ω. A constant output voltage is no longer expected in this case.

IV. Conclusions

The spectral-domain approach is suitable for analyzing the general interconnection of lines in the integrated circuit. It gives frequency-dependent information about the propagation characteristics, and the derived 4-port equivalent-network parameters are more accurate and useful than the conventional lumped-element model. This method is general and can be easily extended to the multiconductor case.

References

[1] T. Sakurai, "Approximation of wiring delay in MOSFET LSI," *IEEE J. Solid-State Circuits*, vol. SC-18, no. 4, pp. 418–426, Aug. 1983.

[2] H.-T. Yuan, Y.-T. Lin, and S.-Y. Chiang, "Properties of interconnection on silicon, sapphire, and semi-insulating gallium arsenide substrates," *IEEE J. Solid-State Circuits*, vol. SC-17, no. 2, pp. 269–274, Apr. 1982.

[3] J. Chilo and T. Arnaud, "Coupling effects in the time domain for an interconnecting bus in high-speed GaAs logic," *IEEE Trans. Electron Devices*, vol. ED-31, pp. 347–352, Mar. 1984.

[4] P. Kennis and L. Faucon, "Rigorous analysis of planar MIS transmission lines," *Electron. Lett*, vol. 17, no. 13, pp. 454–456, June 1981.

[5] D. Mirshekar-Syahkal and J. B. Davies, "An accurate, unified solution to various fin-line structures, of phase constant, characteristic impedance, and attenuation," *IEEE Trans. Microwave Theory Tech.*, vol. MTT-30, pp. 1854–1861, Nov. 1982.

[6] T. Itoh, "Spectral-domain immittance approach for dispersion characteristics of generalized printed transmission line," *IEEE Trans. Microwave Theory Tech.*, vol. MTT-28, pp. 733–736, July 1980.

[7] R. Jansen, "Unified user-oriented computation of shielded covered and open planar microwave and millimeter-wave transmission-line characteristics," *Inst. Elec. Eng. J. Microwave, Optics and Acoustics*, vol. 3, no. 1, pp. 14–22, Jan. 1979.

[8] V. K. Tripathi, "Assymetric coupled transmission lines in an inhomogeneous medium," *IEEE Trans. Microwave Theory Tech.*, vol. MTT-23, pp. 734–739, Sept. 1975.

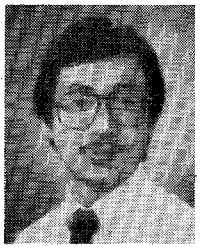

Yoshiro Fukuoka (S'81–M'84) was born in Osaka, Japan, in October 1956. He received the B.S. degree and the M.S. degree from the University of Electro-Communications in 1979 and 1981, respectively. He received the Ph.D. degree from the University of Texas at Austin in 1984. He then joined Uniden Satellite Technology in August 1984, where he is currently working on TVRO systems. His current research interests are in printed circuit components and microwave and millimeter-wave integrated circuits.

Qiu Zhang was born on the 19th of October, 1941, in Jiang Xi, China. After graduating from the Third High School in Nan Chang, he entered the Jiang Xi University in 1961 and graduated in 1966.

From 1967 to 1979, he was an Assistant Engineer in the Nan Chang Hard Alloy Factory. Since 1980, he has been employed as an Engineer in the Information Institute of Science and Technology of Jiang Xi Province. In September of 1981, he began graduate studies at the University of Texas at Austin under the supervision of Prof. Tatsuo Itoh. He received the degree of Master of Science in Engineering from that institution in May of 1984.

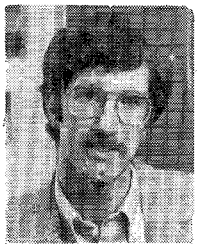

Dean P. Neikirk (S'81–M'83) was born in Oklahoma City, OK, on October 31, 1957. He received the B.S. degree (1979) in physics from Oklahoma State University, and the M.S. (1981) and Ph.D. (1984) degrees in applied physics from the California Institute of Technology.

He joined the faculty of the University of Texas at Austin in 1984, and is currently Assistant Professor in the Department of Electrical and Computer Engineering. His research interests include far-infrared imaging systems, device structures for monolithic microwave integrated circuits, and advanced integrated circuit processing techniques. He has developed a new teaching laboratory for solid-state device fabrication at the University of Texas, and is an active member of the University of Texas Microelectronics Research Center. In 1984, he received the Marconi International Fellowship Young Scientist Award "for contributions to the development of millimeter wave integrated circuits especially in the area of detectors and imaging arrays."

Tatsuo Itoh (S'69–M'69–SM'74–F'82) received the Ph.D. degree in electrical engineering from the University of Illinois, Urbana, in 1969.

From September 1966 to April 1976, he was with the Electrical Engineering Department, University of Illinois. From April 1976 to August 1977, he was a Senior Research Engineer in the Radio Physics Laboratory, SRI International, Menlo Park, CA. From August 1977 to June 1978, he was an Associate Professor at the University of Kentucky, Lexington. In July 1978, he joined the faculty at the University of Texas at Austin, where he is now a Professor of Electrical and Computer Engineering and Director of the Electrical Engineering Research Laboratory. During the summer 1979, he was a Guest Researcher at AEG-Telefunken, Ulm, West Germany. Since September 1983, he has held the Hayden Head Centennial Professorship of Engineering at the University of Texas.

Dr. Itoh is a member of the Institute of Electronics and Communication Engineers of Japan, Sigma Xi, and Commission B of USNC/URSI. He serves on the Administrative Committee of the IEEE Microwave Theory and Techniques Society and is the Editor of the IEEE TRANSACTIONS ON MICROWAVE THEORY AND TECHNIQUES. He is a Professional Engineer registered in the State of Texas.